Modeling the acoustic radiation of plates using circular pistons

Carlos García A.[a], Nicolas Dauchez[a] and Gautier Lefebvre[a]

[a]*Université de technologie de Compiègne, Roberval (Mechanics, energy and electricity), Centre de recherche Royallieu - CS 60319 - 60203 Compiègne cedex, France*

ARTICLE INFO

Keywords:
Equivalent piston model
Average radiation efficiency
Mean radiated power
Complex-shaped plates
Tetris plates
Hear the shape of a drum

Abstract

We propose an equivalent piston model (EPM) for estimating the modal radiation efficiency of complex-shaped plates. The model is based on a spatial distribution of equivalent pistons that emulates how each mode radiates sound. For shapes close to a rectangle, a specific version of the method is proposed by representing the shape only by two dimensions (EPM-RD). The validity of this assumption is evaluated in terms of shape dissymmetry, which can cause residual radiators to appear, and where the dissymmetry can affect the spatial distribution of lobes. With a known spatial distribution mimicking the mode shapes, it is possible to estimate also average values of the radiation parameters, such as the average radiation efficiency and average power. The average radiation efficiency and power follow the Equipartition Theorem and allow the calculation to be performed without the cross-terms and using only the modal efficiencies and the resonance frequencies. Due to their simplicity and ease of implementation, piston-based equivalent models have the great potential for solving radiation problems from flat structures. In principle, any mode shape can be modeled with vibrating pistons since analytical formulations are provided regardless of volume velocities, phases, or positions of the pistons. Moreover, average values can also be calculated, such as with EPM-RD, which provides an approximate estimate of average radiated properties within seconds without requiring any integration or large matrices to be solved.

1. Introduction

Several decades have been spent studying the vibration and radiation of planar structures. The pioneering works of Rayleigh [1], Maidanik [2] and Leissa [3] paved the way for understanding vibration and radiation of flat structures, paying particular attention to the radiation resistance and efficiency of rectangular [4] and circular [5] plates, with simply supported, clamped [6] or general boundary conditions [7]; with or without the presence of a baffle [8]. In general, acoustic radiation can be categorized into two types depending on the excitation characteristics. In the first category, the modes are excited unevenly, and the acoustic response is determined by the characteristics of the excitation. Punctual forces and plane waves hitting structures at grazing angles are examples of this. In this case, cross-modal radiation must be taken into account in order to calculate the sound power, and omitting it may result in higher or lower radiated power [9]. While modal coupling has little effect on the power of a plate when excited above resonance, it can become significant under off-resonant excitation [10] and if more than one mode is excited at the same time, the total power cannot be calculated as a sum of all modes [11, p. 409]. In the second category, the acoustic response become independent of the characteristics of the excitation. This can be seen in diffuse fields, turbulent boundary layer (TBL) and rain on roof (ROFs) excitations. As a result of the orthogonality of the modal eigenfunctions, the effects of modal coupling tend to disappear [12, p. 328]. In light of this argument, Xie et al. [13] calculated the average radiation efficiency of a simply supported plate by integrating over all the possible punctual positions, using the modal radiation efficiency of a simply supported plate given by Maidanik and Wallace [4, 14].

The equations describing the radiation, even for the simplest cases, i.e. the rectangular simply supported or circular clamped plate, do not have canonical solutions, so they must be expanded in a sum series [15, 16, 6] or solved numerically. Adding a small amount of complexity to the geometry render analytical solutions impossible. It is necessary then to use numerical tools, such as the finite element method (FEM), boundary element method (BEM), coupled FEM and BEM or semi-analytical approaches that match the boundary conditions, such as Rayleigh-Ritz method. To avoid this, equivalent sources can be used to simulate the radiation of structures. This is not a new concept; for example, Cremer and Heckl [12, p. 512] decomposed a mode shape into point sources. Other equivalent radiators considered were squared pistons [2], spherical sources [17] or radiation modes [18]. According to Rdzanek [6], any

ORCID(s):

circular surface source, including pistons, membranes, and plates can replace the source's vibration velocity distribution valid for a clamped circular plate.

In this paper, we use a collection of elementary circular piston radiators to simulate mode shape patterns to determine the modal and average radiation efficiency of flat structures with various regular and irregular shapes. This work is based on the approach of García A. et al. [19] who proposed a method to calculate far-field radiation from circular pistons vibrating with arbitrary phases, sizes, and positions. A specific version of the method consist in finding a equivalent rectangular shape with two characteristic lengths given by the inertia tensor, and the pistons are distributed in rectangular arrays. The approximated modal radiation agrees well below the coincidence frequency. Moreover, it explains well not only the low-limit radiation in "edge" and "corners" modes but also the transitions, e.g. from monopolar into dipolar radiation, in simple cases and how the plate's shape affects the radiation. This method considers only the plate's geometry and the resonance frequencies. The average radiation efficiency and mean power can therefore be calculated without any further integration or large matrices.

This paper is organized as follows: in Section 2, the main descriptors used to characterize the radiation of baffled plates vibrating in light-fluids are given. In Section 3, we present the equivalent piston model (EPM) and how to define the characteristics of the equivalent pistons. In Section 4, the EPM is used with a rectangular distribution of the pistons (EPM-RD). An equivalent rectangular surface is used determine the piston's position and size automatically for every mode. This allows us to extend the method from the modal radiation into the average radiation of complex-shaped structures "close" to rectangles, and the main characteristics and limitations are tested on a variety of plate shapes.

2. Acoustic radiation of flat structures

2.1. Baffled plates

The Kirchhoff-Helmholtz integral can be used to calculate the pressure at any point given a normal velocity field $\hat{v}$. When considering a baffled plate, choosing a Green's function that cancels at the baffle boundary leads to Rayleigh's integral

$$\hat{p}(\mathbf{r}) = \frac{j\omega\rho_0}{2\pi} \iint_S \frac{e^{jk\|\mathbf{r}-\mathbf{r_0}\|}}{\|\mathbf{r}-\mathbf{r_0}\|} \hat{v}\,\mathrm{d}S, \tag{1}$$

where the characteristic impedance of the medium is $\rho_0 c$, for a medium with density ρ and speed of sound c; $\mathbf{r_0}$ is the vector spanning the plate's surface, $k = \omega/c$ the acoustic wavenumber and $j = \sqrt{-1}$. The Rayleigh integral relates the far-field radiation from planar sources to the Fourier transform of their surface velocity and is one of the fundamental equations in acoustic radiation. The averaged power can be calculated when the pressure is integrated over a hemisphere of surface S^h as

$$\mathcal{P}(\omega) = \frac{1}{\rho_0 c} \iint_{S^h} |\hat{p}(\mathbf{r})|^2 \mathrm{d}S. \tag{2}$$

Wallace [4], Gomperts [20], Bouwkamp [21], Donato [22] and Dym [23] used this definition to express the analytical solution for a rectangular plate. This can also be achieved by averaging the complex conjugate of the normal velocity $\hat{v}^\star$ and the parietal pressure over the vibrating structure's surface S

$$\mathcal{P}(\omega) = \frac{1}{2} \iint_S \mathrm{Re}\Big\{ \hat{p}(\mathbf{r_0}) \cdot \hat{v}^\star(\mathbf{r_0}) \Big\} \mathrm{d}S. \tag{3}$$

Numerous authors have chosen this approach for computing the radiated power since the integration takes place at the surface of the structure [15, 24, 25, 6]. Inserting Eq. (1) into Eq. (3) and expanding the velocity into a sum of m modes, acoustic power can be expressed in terms of structural modes, $\hat{v} = \{\boldsymbol{\phi}\}^\intercal\{\hat{\mathbf{v}}\}$ where the column vector $\{\hat{\mathbf{v}}\} = [\hat{v}_1, \hat{v}_2, \ldots, \hat{v}_m]$, the row vector containing the modes $\{\boldsymbol{\phi}(\mathbf{r_0})\} = [\phi_1(\mathbf{r_0}), \phi_2(\mathbf{r_0}), \ldots, \phi_m(\mathbf{r_0})]$, and $\intercal$ stands for the vector's transpose. Similarly, by discretizing the structure into small sections, i.e. elementary radiators, the power can also be expressed as a sum of the vibrations of each radiator and the parietal pressure, calculated with the acoustic radiation resistance matrix (ARM) and the vector velocities of the elements $\{\hat{\mathbf{v}}_\mathbf{e}\} = [\Psi]\{\hat{\mathbf{v}}\}$. Hence [26, p. 161],

$$\begin{aligned}\mathcal{P}(\omega) &= \frac{\omega\rho_0}{4\pi}\{\hat{\mathbf{v}}\}^{\mathrm{H}}\left(\iint_S\iint_S\{\boldsymbol{\phi}(\mathbf{r_0})\}^{\intercal}\frac{\sin(k\|\mathbf{r}-\mathbf{r_0}\|)}{\|\mathbf{r}-\mathbf{r_0}\|}\{\boldsymbol{\phi}(\mathbf{r_0}')\}\,\mathrm{d}S'\,\mathrm{d}S\right)\{\hat{\mathbf{v}}\}\\ &= \{\hat{\mathbf{v}}\}^{\mathrm{H}}[\mathbf{A}(\omega)]\{\hat{\mathbf{v}}\}, \qquad \text{in terms of structural modes}\\ &= \{\hat{\mathbf{v}}\}^{\mathrm{H}}[\Psi^{\mathrm{H}}][\mathbf{R}][\Psi]\{\hat{\mathbf{v}}\}, \quad \text{in terms of elementary radiators.}\end{aligned} \tag{4}$$

$[\mathbf{A}(\omega)]$ is commonly called the Power Transfer Matrix, analytical solutions for the rectangular case are found in [27, 16] and $\{\mathbf{z}\}^{\mathrm{H}}$ is the Hermitian transpose of the vector $\{\mathbf{z}\}$. The quadruple integral in the Power Transfer Matrix can be avoided by using the elementary radiator's approach, but the accuracy is frequency-limited by the squared number of elements and large matrices may need to be stored. $[\mathbf{R}]$ is the acoustical radiation resistance matrix, whose coefficients can be calculated using a discrete version of Rayleigh's integral [26, 28]. Hashimoto [29] presented another approach using equivalent circular pistons, called the discrete calculation method (DCM), in which AMR's coefficients are

$$\begin{aligned}R_{ii} &= \rho_0 c S_i\left(1-\frac{J_1(2ka_i)}{ka_i}\right),\\ R_{ij} &= \frac{2\rho_0 c k^2 S_i S_j}{\pi}\left(\frac{J_1(ka_i)}{ka_i}\frac{J_1(ka_j)}{ka_j}\right)\operatorname{sinc}(kd_{ij})\end{aligned} \tag{5}$$

and where the notation ij refers to a pair of pistons of radii $a_{i,j}=\sqrt{S_{i,j}/\pi}$ separated a distance d_{ij}. J_n is the Bessel function of the first kind of n order and $\operatorname{sinc}(x)=\sin(x)/x$. In the case of a plate vibrating in light-fluid, vibration and radiation problems can be decoupled. As a rule of thumb, this occurs when $\rho_0/k\rho_s \ll 1$ [30], where ρ_s is the surface density of the plate.

2.2. Average values of the mean-square velocity

A harmonic force $\hat{f} = Fe^{j\omega t}$ generates kinetic energy depending on where it is applied. For a plate with homogeneous distribution of the mass $\rho(\mathbf{r_0})=\rho$, uniform thickness h, $M=S\rho h$ and homogeneous damping η, it is straightforward to average the mean-square velocity over all possible punctual positions, which results in an average value independent of the modal mass and excitation position. Hence, the time average of the spatial average mean-square velocity, averaged then over all possible force positions is [13]

$$\overline{\langle\bar{v}^2\rangle} = \frac{1}{S}\iint_S\langle\bar{v}^2\rangle\mathrm{d}x_0\mathrm{d}y_0 = \sum_m^{\infty}\frac{|F|^2}{2M^2}\frac{\omega^2}{(\omega_m^2-\omega^2)^2+\eta^2\omega_m^4}. \tag{6}$$

For simplicity, we will refer to this parameter as average mean-square velocity. Further, the mean-square velocity, or, for formality's sake, the time average of the spatial average mean-square velocity is [31, p. 11]

$$\langle\bar{v}^2\rangle = \frac{1}{S}\iint_S\frac{|v^2|}{2}\mathrm{d}S \tag{7}$$

in the case of harmonic oscillations and the spatial mean-square of the velocity $\bar{v}^2$ corresponds also to the kinetic energy of the system divided by the overall mass [12, p. 327].

2.3. Radiation efficiency

The radiation efficiency is a dimensionless parameter used to describe the acoustic performance of structures. It is defined physically as the ratio of the radiated acoustic power over a reference power $\sigma=\hat{\mathcal{P}}/\hat{\mathcal{P}}_0$ [32], where $\hat{\mathcal{P}}_0$ is commonly the mechanical power driven by a piston vibrating at the same mean-square velocity

$$\sigma = \frac{\mathcal{P}(\omega)}{\rho_0 c S\overline{\langle\bar{v}^2\rangle}}. \tag{8}$$

2.3.1. Modal radiation efficiency σ_m

Using a modal formalism, Eq. (8) also defines the modal efficiency and modal power. Below the coincidence frequency $k_p = k$, where k_p is the plate's wavenumber, the modal radiation efficiency of the first modes can be spotted by their slope. The slope is proportional to the $2(m + 1)$ power of ka in circular cases, where m is to the number of concentric circular nodal lines [5]. In rectangular cases, the slope is proportional to the $2(m + n - 1)$ power; m, n corresponds to the modal indices (see also Table 2). Using DCM or EPM, above the coincidence frequency, convergence to one is expected due to the use of pistons.

In any case, the first mode radiates as a monopole, with a slope of 6 dB/octave. The next mode is expected to be a dipole disposed along the larger length and presenting a slope of 12 dB/octave. Afterwards, even for simple geometries, it becomes difficult to predict which mode will appear. According to Euler-Lagrange's principle of minimal energy, lower order modes will appear before higher order modes. Usually, this occurs alongside two characteristic lengths, such as in a rectangular plate, but following the natural axis of coordinates for each structure, such as circular plates with polar coordinates and elliptical plates with elliptic coordinates. Identifying the axes for arbitrary shapes is still is an open question.

Increasing the mode order leads to oscillations in modal radiation efficiency and the literature in this area is vast. Maidanik [2], for example, states that modes can be classified according to where they lie in the k-space: corners, edges, and surfaces modes (also in [33, p. 70] and in [34]): the side to side lobes in the mode shapes cancel each other out, and the remainder radiation is "governed" by the remaining most distant non-cancelled lobes, which tend to increase radiation proportionally to their virtual surfaces and distances. Radiation of edges occurs when the remainder of non-cancelled lobes are disposed on opposite edges, presenting monopolar or dipolar characteristics depending on their phase. While this is true at low frequencies, the way the mode radiates changes as the frequency increases. Even if these oscillations in modal efficiencies are well known, there have been few attempts to describe them in detail, perhaps because there are no simple analytical formulations available.

2.3.2. Radiation efficiency due to punctual excitations σ

Figure 1 shows the radiation efficiency of ten random positions, the mean radiation averaged over the ten positions as well as the average radiation efficiency. No matter the plate shape, similar behavior is to be expected under a light-fluid assumption, whether they are circular, rectangular, elliptical, etc. Radiation efficiency is affected by the excitation position within the structure, but global trends can still be observed.

Below the first resonance, the plate radiates as a monopole, whether it is clamped or simply supported (see [6] for circular cases). The radiation efficiency then drops in presence of zero-flux modes due to the average velocity of the plate tending to zero, as well as the stiffer slope depending on the radiation type (dipole, quadrupole, etc.). Afterwards, radiation is mainly governed by edge and corner modes [26, p. 190], [34, p. 44]. Because the radiation depends on the excitation force's position, large variations may be observed in this zone. As shown in Fig. 1 radiation efficiency is also proportional to damping; increasing the damping also increases the radiation efficiency (see also [35]). Radiation efficiency peaks just afterwards the critical frequency f_c [36]. Above the critical frequency, radiation efficiency is not influenced by the damping factor [35] and decays asymptotically to 4/3 and 9/5 in simply supported and clamped circular radiators [37, 38], a lower value than $(1 - L_x^2 - L_y^2)^{-1/2}$ stated by Wallace [14] and F. G. Leppington et al. [39] for rectangular plates with simply supported boundaries. Radiation efficiency depends on the boundary conditions also below the critical frequency. In this zone, there is a 3 dB increase in radiation efficiency when the plate is clamped [40], or twice as much as when it is simply supported [41, p. 150]. However, this holds true for higher modes and not for the first modes [42]. A plate with a combination of simply supported and clamped edges has almost the same radiation efficiency as a simply supported plate (difference < 1 dB) [20].

2.3.3. Average radiation efficiency $\bar{\sigma}$ and mean power

The average radiation efficiency can be determined independently of the excitation position by considering all possible force positions. As a consequence, "every mode of vibration [is] alike favored", as Rayleigh [43] used to call the equipartition theorem, giving a global overview of the plate's efficiency. The average radiation efficiency can be

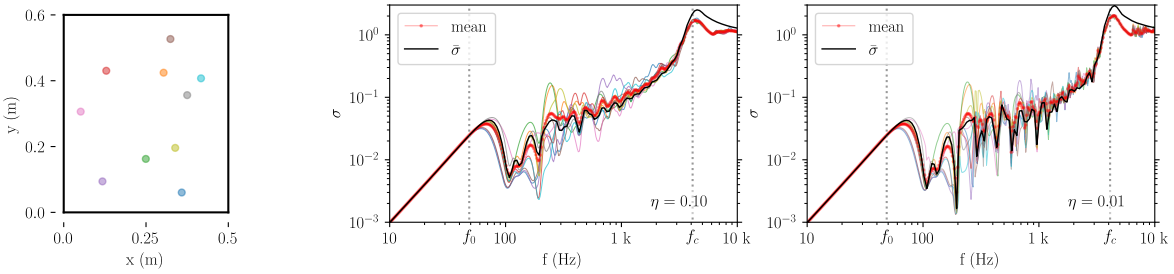

Figure 1: a) Simply supported rectangular plate excited at ten random positions (colored dots). b) Analytical average radiation efficiency (solid black lines ——) and the mean of the efficiencies calculated with DCM (solid-dotted red lines —•—) for two damping factors $\eta = 0.1$ and $\eta = 0.01$.

calculated as [13]

$$\bar{\sigma} = \frac{\sum_{m}^{\infty} \sigma_m \langle \bar{v}_m^2 \rangle}{\langle \overline{\bar{v}^2} \rangle} = \frac{\sum_{m=1}^{\infty} \sigma_m \left[\left(\omega_m^2 - \omega^2 \right)^2 + \eta^2 \omega_m^4 \right]^{-1}}{\sum_{m=1}^{\infty} \left[\left(\omega_m^2 - \omega^2 \right)^2 + \eta^2 \omega_m^4 \right]^{-1}}. \tag{9}$$

Note that, due to mode orthogonality, modal mutual efficiencies disappear and the average radiation efficiency is directly related to the mode resonance frequencies ω_m and their modal radiation efficiencies σ_m. Usually, the largest variations occur when the mode overlap is small and the influence of each mode is significant [9], which is greatly dependent upon the shape of the plate. Using the modal approach, the reader must be aware that one must not only perform a modal analysis of the entire structure, but must also calculate the radiation of each mode individually and sum them up, which can take a long time. However, Eq. (9) also shows that it is not necessary to know the exact modal shapes to determine average radiation efficiency, but rather how each mode radiates sound.

The radiated mean power can then be written, according to Eqs. (8) and (9), as

$$\bar{\mathcal{P}}(\omega) = \bar{\sigma} \rho_0 c S \langle \overline{\bar{v}^2} \rangle. \tag{10}$$

2.4. Case study: Can one hear the shape of a drum?

The mean radiated power, efficiency and mean-square velocity can be used, for example, to answer the famous question raised in 1966 by Kac [44]: *Can one Hear the Shape of a Drum?*, or as he quoted form Bergs: “You mean, if you had perfect pitch could you find the shape of a drum”. This question emerged after describing two eigenvalue problems and asking if there are two regions that are congruent in the sense of Euclidean geometry. Gordon [45, 46] formally responded no, arguing that two geometries can be isospectral, suddenly closing the debate. Sridhar and Kudrolli [47] measured the first 54 eigenfrequencies of two cavities with membranes whose geometry was described by Gordon. Even though the eigenvalues were the same, confirming the isospectrality of the shapes, the measured vibration amplitude differed. This was “irrelevant” to them, since, quoting Sridhar and Kudrolli "the phrase hearing the shape of drums is conventional to refer only to the eigenvalue spectrum, independent of the amplitude of excitation.” But in order to not hearing the shape of the “drum” (membrane, plate, or any other type of structure) we think the goal must be to find two geometries that emit equal radiated pressure and power, not just geometries that contain the same spectrum. As seen in Fig. 3, both plates have the same average mean-square velocity, due to isospectrality (see Eq. (6)). DCM is used to calculate the modal and average radiated efficiency, as well as the mean radiated power. Taking the second mode (Fig. 2b) as a example, drum 1 radiates as a monopole and drum 2 as a dipole. This particular mode affect the radiation of the whole structure. The second mode of drum 1 radiates as a monopole even if its the second mode, due to localization [48], adding another layer of complexity when predicting the radiated power and efficiency of complex plates. You may or may not be able to reconstruct the shape of the plate, but might clearly hear the difference between the isospectral geometries presented by Gordon.

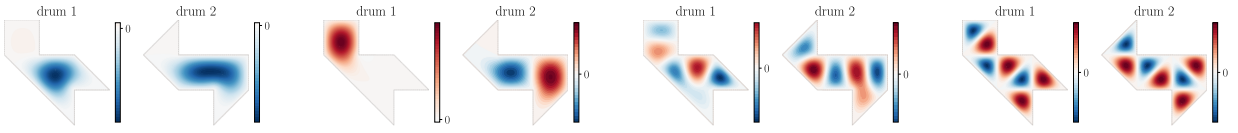

(a) N=1 (b) N=2 (c) N=6 (d) N=9

Figure 2: Mode shapes of isospectral plates. Both plates have the same eigenfrequencies for any N mode.

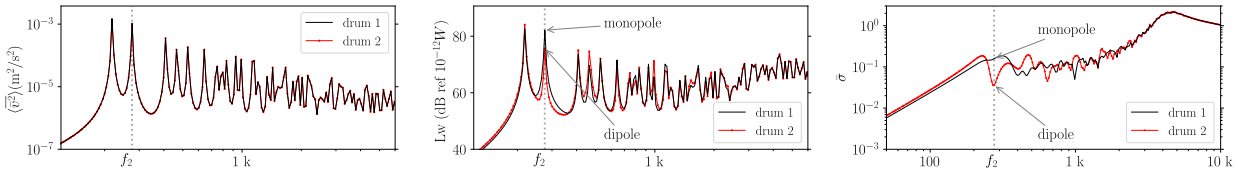

(a) Average mean-square velocity (b) Mean radiated power (c) Average radiation efficiency

Figure 3: Radiation of isospectral plates. The second mode (N=2) has a resonance frequency of $f_2 = 275.63$ Hz and radiates as a monopole for "drum 1", and as a dipole for "drum 2".

The use of a modal approach may be valuable for complex plates, but, the large matrices required to calculate the radiation, make its practical implementation cumbersome (see [49]). This difficulty can be avoided by using equivalent radiators, as described in the next section.

3. Equivalent piston model (EPM)

In the equivalent piston model, each mode shape is to be simulated as a distribution of circular pistons vibrating in phase or in phase opposition. A similar approach was previously considered using equivalent point sources instead of pistons by Cremer and Heckl [12] to calculate the radiated pressure of a mode, but since there is no equivalent definition of radiation efficiency similar to Eq. (8) for point-source distributions [50], it is not possible to estimate the radiation efficiency of the structure in that manner. The radiated power of each lobe is calculated as a single vibrating piston and the interactions between lobes are described by the mutual radiation impedance of each pair of pistons. The far-field radiated power is governed only by the real part of the impedance, so only the radiation resistance will be considered at this stage. By incorporating the volume velocity into the piston distribution model presented by García A. et al. [19], any mode can be modeled by a collection of pistons with piston dimensions derived by geometrical means. Using a proper distribution for modeling higher-order modes enables the method to estimate also average values of radiation efficiency.

3.1. Modal radiation analogous to vibrating pistons

Consider N pistons with radii a_l, $l = 1, 2, \ldots, N$ and phases $\Phi_l \in (0, 2\pi]$ as in Fig. 4. Vector $\mathbf{r}_j$ represents the position and vector $\mathbf{k}$ a vector from each piston center. The volume velocity of one piston is $\hat{Q}_l = \pi a_l^2 \hat{V}_l$, where $\hat{V}_l$ is the harmonic velocity. The generated pressure of such distribution of pistons is

$$\hat{p}(\mathbf{r}) = \frac{jk\rho_0 c}{2\pi r} \sum_{l=1}^{N} \hat{Q}_l D_l(\mathbf{k}) e^{j(\mathbf{k}\cdot\mathbf{r}_l + \Phi_l)} \tag{11}$$

and piston's directivity

$$D(\theta, \phi) = \frac{2J_1(ka\sin\theta)}{ka\sin\theta}. \tag{12}$$

Using the bridge product theorem [51, p. 699] or first product theorem for arrays [33, p. 49] and due to circular symmetry of the sources, the specific radiation resistance and efficiency of any distribution of pistons can be calculated

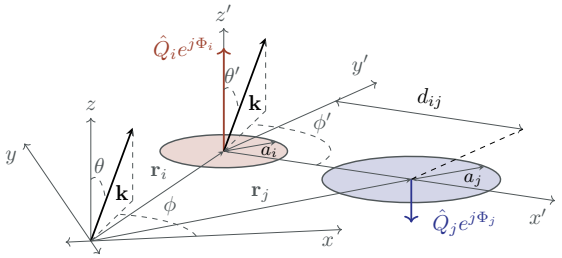

Figure 4: Pistons with different volume velocities on the plane xy. The bridge theorem is used to construct the directivity pattern and Bouwkamp's impedance theorem is employed to calculate the radiation resistance and efficiency of any distribution of pistons [19].

by integrating the modulus of the squared directivity over a hemisphere, regardless the phase, size and position of the pistons on a baffled plane xy [19]. Including the volume velocity in the model presented by García A. et al. [19], the total power, according to Eq. (2), is

$$\begin{aligned}\mathcal{P}(\omega) &= \frac{1}{\rho_0 c}\int_0^{2\pi}\int_0^{\frac{\pi}{2}} \frac{|\hat{p}(\mathbf{r})|^2}{2} r^2 \sin\theta \mathrm{d}\theta \mathrm{d}\phi \\ &= \frac{k^2\rho_0 c}{8\pi^2}\int_0^{2\pi}\int_0^{\frac{\pi}{2}} \left(\sum_{l=1}^{N} \hat{Q}_l^2 \frac{4J_1^2(ka_l\sin\theta)}{k^2 a_l^2 \sin^2\theta} \right. \\ &\left. + 2\sum_{i=1}^{N}\sum_{j>i}^{N} \hat{Q}_i\hat{Q}_j \frac{2J_1(ka_i\sin\theta)}{ka_i\sin\theta}\frac{2J_1(ka_j\sin\theta)}{ka_j\sin\theta}\cos(kd_{ij}\sin\theta\cos\phi+\Phi_{ij}) \right)\sin\theta\mathrm{d}\theta\mathrm{d}\phi \\ &= \frac{\rho_0 c}{2}\left(\sum_{l=1}^{N} a_l^2\hat{V}_l^2\sigma_p(a_l) + 2\sum_{i=1}^{N}\sum_{j>i}^{N} a_i a_j \hat{V}_i\hat{V}_j\sigma_{2p}(a_i,a_j,d_{ij},\Phi_{ij}) \right),\end{aligned} \tag{13}$$

where $\sigma_p(a_l)$ is the self-radiation efficiency of piston l; d_{ij} is the distance, Φ_{ij} the relative phase and σ_{2p} is the mutual-radiation efficiency between each pair of pistons ij respectively. Dividing the acoustic power to the reference time average power $\hat{\mathcal{P}}_0 = \rho_0 c \sum_l S_l \hat{V}_l^2/2$, the radiation efficiency is calculated as

$$\sigma = \frac{1}{\sum_l a_l^2\hat{V}_l^2}\left(\sum_{l=1}^{N} a_l^2\hat{V}_l^2\sigma_p(a_l) + 2\sum_{i=1}^{N}\sum_{j>i}^{N} a_i a_j \hat{V}_i\hat{V}_j\sigma_{2p}(a_i,a_j,d_{ij},\Phi_{ij}) \right). \tag{14}$$

When pistons of equal size are considered, Eq. (14) can be simplified further as

$$\sigma = \frac{1}{\sum_l \hat{V}_l^2}\left(\sum_{l=1}^{N} \hat{V}_l^2\sigma_p(a_l) + 2\sum_{i=1}^{N}\sum_{j>i}^{N} \hat{V}_i\hat{V}_j\sigma_{2p}(a,d_{ij},\Phi_{ij}) \right). \tag{15}$$

This equation will be used in Section 4.6.1. Additionally, if all pistons are all driven at the same velocity,

$$\sigma = \sigma_p(a_l) + \frac{2}{N}\sum_{i=1}^{N}\sum_{j>i}^{N}\sigma_{2p}(a,d_{ij},\Phi_{ij}). \tag{16}$$

The self-radiation efficiency $\sigma_p(a)$ is the radiation efficiency of a circular piston of radius a,

$$\begin{aligned}\sigma_p(a) &= 1 - \frac{J_1(2ka)}{ka} \\ &= \frac{(ka)^2}{2} - \frac{(ka)^4}{2^2\cdot 3^1} + \frac{(ka)^6}{2^4\cdot 3^2}\cdots\end{aligned} \tag{17}$$

and the mutual-radiation efficiency σ_{2p} describes how the radiated pressure of each piston affects other pistons in the distribution. This effect is not solely influenced by piston size or effective area, but also by the distances d_{ij} and phases Φ_{ij} between each pair of pistons. The mutual efficiency for a pair of pistons ij can be calculated as [19]

$$\begin{aligned}\sigma_{2p}(a_i, a_j, d_{ij}, \Phi_{ij}) = \frac{2}{\sqrt{\pi}} \sum_{p=0}^{\infty} \sum_{q=0}^{\infty} \left(\frac{a_i}{d_{ij}}\right)^p \left(\frac{a_j}{d_{ij}}\right)^q \frac{J_{m+1}(ka_i) J_{n+1}(ka_j)}{p!q!} \Gamma\left(p+q+\frac{1}{2}\right) \\ \times \left[j_{p+q}(kd_{ij}) \cos\Phi_{ij} + \mathbf{h}_{p+q}(kd_{ij}) \sin\Phi_{ij}\right],\end{aligned} \tag{18}$$

where the gamma function of a positive half-integer is defined for any $n \in \mathbb{Z}^+$ as $\Gamma(n+1/2) = \sqrt{\pi}/2^n(2n-1)!$ and j_n and $\mathbf{h}_n$ are the spherical Bessel and Struve functions of the first kind of order n respectively. Considering two pistons of equal size vibrating in phase or in phase opposition, using the first three terms of Eq. (18) yields to

$$\sigma_{2p}(a, d) \simeq \pm 2\left(J_1^2(ka) + \frac{a}{d}\Upsilon J_1(ka) J_2(ka) + \left(\frac{a}{d}\right)^2 \Lambda J_2^2(ka)\right) \mathrm{sinc}(kd), \tag{19}$$

in which $\Upsilon = 1/kd - \cot(kd)$ and $\Lambda = 3/4(3\Upsilon/kd - 1)$, and the sign $+$ is relates a couple of pistons vibrating in phase, and $-$ for the opposite case.

Equation (18) can be analyzed similarly for pistons vibrating in phase; if the distance between a pair of pistons is larger than their radii, one finds the mutual coefficients $\boldsymbol{R}_{ij}$ of the radiation resistance matrix (see Eq. (5)).

3.2. Equivalent radius of radiation

The aim is to determine the radius of the piston that will radiate as a single lobe within a mode shape. Then, each lobe can be considered as a simply supported plate, with boundaries that match the modal lines. As a first step towards recreating the radiation of the first mode of a simply supported plate with arbitrary shape, let's begin by linking two circular geometries: the simply supported flexural disk and a circular piston.

Greenspan [38] calculated the radiated power of different types of circular radiators, and proposed a method applicable not only to piston cases but also to simply supported and clamped radiator. He showed that the low frequency behavior in the three cases is proportional to $(ka)^2/2$ with a factor given by the total volume velocity $\hat{Q}$. As frequency increases, however, the radiated efficiency of circular radiator convergences to 1 for pistons, 4/3 for simply supported radiators and to 9/5 for clamped radiator. If the radiators have the same flux, it is possible to match the low frequency behavior between pistons and other circular radiators, re-scaling the efficiency of the simply supported disk to match that of the piston. Consider, for instance, the volume displaced by a piston $\hat{Q}_p$ with radius a_p and the volume velocity $\hat{Q}_s$ of the first mode of a circular plate with radius a_s with clamped boundaries. The result of equating $\hat{Q}_p$ and $\hat{Q}_s$,

$$\int_0^{a_p} \int_{-\pi}^{\pi} r \mathrm{d}r\mathrm{d}\theta = \int_0^{a_s} \int_{-\pi}^{\pi} \left(J_0(\chi_{01} r/a_s) - \frac{J_0(\chi_{01})}{I_0(\chi_{01})} I_0(\chi_{01} r/a_s)\right) r \mathrm{d}r\mathrm{d}\theta, \tag{20}$$

where χ_{01} is the first zero of $J_0(x)$ and $I_n(x)$ is the modified Bessel function of the first kind, leads to an equivalence between radii a_p and a_s. Re-scaling the radiated efficiency to match the behavior of a piston gives

$$C = \frac{4}{3}\sqrt{\frac{2J_1(\chi_{01})}{\chi_{01}}}. \tag{21}$$

For a simply supported radiator, $a_{eq} = a_s C$ gives the *equivalent radius of radiation*, where $a_s = \sqrt{S/\pi}$ and S represents the surface of a lobe in the mode shape. We may now follow the same procedure for an arbitrary shaped plate, i.e. to match the radiation of the fist mode with that of a circular piston. It may be possible to find an equivalent radius based on the geometric information of the structure, such as its surface S and perimeter P. The idea of finding an equivalent radius based on the surface and perimeter was first presented by Mechel (1989), who linked the specific impedance of air plugs in Helmholtz resonators to that of circular pistons. Moreover, for resonators with non-circular holes, he found experimentally an equivalent effective radius $a_{\text{eff}} \approx 1.06 S^{3/4} P^{-1/2}$ [52, p. 575]. As a result of using

this model of effective radius and including the simply supported radiator-to-piston coefficient, we define the equivalent piston radius as

$$a_{eq} \approx 1.06 C S^{3/4} P^{-1/2}. \tag{22}$$

By knowing the perimeter and the surface of a plate, it is possible to find an equivalent piston that will radiate the same energy into the far-field for the first mode. Furthermore, one can extend this model to higher frequency modes due to the fact that each lobe vibrates as an individual simply supported plate whose boundaries are defined by the nodal lines.

3.3. Location of the pistons

Based on the mode shapes, we may consider locating each piston following the delimited areas enclosed by the nodal lines using the peak of the lobes as a reference point. A generalized model for a plate with arbitrary shape must include automatic positioning of each piston, which can be explored using FEM mode shapes. Alternatively, a geometrical approach to cover a surface with circles that minimize the covered area could be used if these numerical methods are not desired to be employed. Corrective measures can be applied in a second stage if necessary.

3.4. Case study: Tetris plates

With the piston model, we can treat any mode shape analytically. Four tetris-shaped geometries are shown in Fig. 5, as if they were simply supported thin plates. Mode four (N=4) exhibits four lobes with the same areas and perimeters within each shape. Since the plates are of the same material and thickness, they all have the same resonance frequency, but their radiation efficiency varies. Using Eq. (22), we can determine the piston radii for each square within each mode, and thereby derive analytical equations that describe the modal radiation (see Table 1). Changing the dimensions or materials can change the resonance frequency, but the modal radiation remains the same. By solely changing the position of the pistons to recreate the mode shape, the result is a mode that radiates as a quadrupole (a), two dipolar radiators (b, c) and one monopole-type radiator at low frequencies (d).

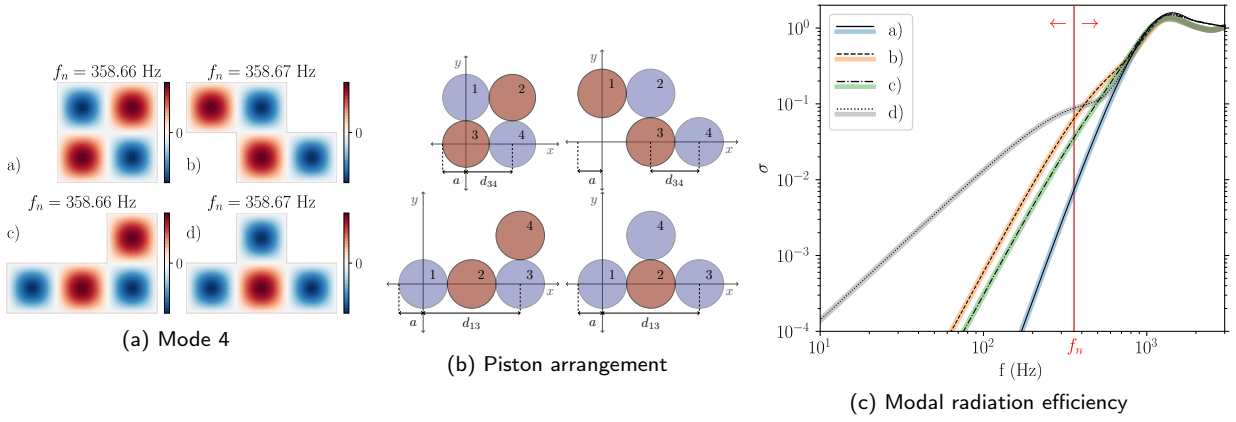

(a) Mode 4 (b) Piston arrangement (c) Modal radiation efficiency

Figure 5: Radiation from Tetris plates. a) Modal analysis shows the same resonance frequency of mode four for all shapes. b) Piston distributions. c) Modal radiation efficiency, calculated with DCM (black lines) and estimated with the EPM (wide colored solid lines). The difference in radiation may vary depending on the tetris shape and the resonance frequency value.

Using this example, we can further strengthen the arguments made in Section 2.4. Several structures may have the same resonance frequency at the same mode (or throughout the spectrum), but the modal radiation may be different depending on the location of their radiating lobes, changing the global radiated sound.

Once the size and position of the pistons are established, the estimation of the modal radiation efficiency is highly accurate. Nevertheless, it may be difficult to generalize this procedure since, a priori, the spatial arrangement of modal lobes is unknown.

Table 1
Analytical radiation efficiency of the mode four in tetris-shaped plates.

Mode	General Equation (28)	ka ≪ 1	Shape
4	$\sigma_p(a) - 2\sigma_{2p}(2a) + \sigma_{2p}(\sqrt{8}a)$	$(ka)^6$	□
4	$\sigma_p(a) - \frac{3}{2}\sigma_{2p}(2a) + \sigma_{2p}(\sqrt{8}a) - \frac{1}{2}\sigma_p(\sqrt{20}a)$	$(ka)^4$	Z
4	$\sigma_p(a) - \frac{3}{2}\sigma_{2p}(2a) + \frac{1}{2}\sigma_{2p}(\sqrt{8}a) + \frac{1}{2}\sigma_{2p}(4a) - \frac{1}{2}\sigma_p(\sqrt{20}a)$	$(ka)^4$	L
4	$\sigma_p(a) - \frac{3}{2}\sigma_{2p}(2a) + \sigma_{2p}(\sqrt{8}a) + \frac{1}{2}\sigma_{2p}(4a)$	$(ka)^2$	T

An simple approach would be to consider a known spatial distribution of pistons, such as in a rectangular plate, and determine whether it is comparable to the actual structure. In other words, under what conditions a rectangular model can be used to estimate the radiation of a plate with complex shape. Once knowing the spatial distribution of pistons, it is possible to extend the EPM to a specialized model that estimate also average values of the radiated power and efficiency.

4. Equivalent piston model - rectangular distribution (EPM-RD)

In this section, we define a spatial distribution of the pistons in a rectangular array and use the EPM to calculate the radiated efficiency of such array. This use of the EPM with a rectangular distribution of pistons will be called EPM-RD. Since the lobes in the modes in rectangular geometries are arranged in symmetric arrays, it is straightforward to determine the center positions of the lobes for each mode, where piston will be located. Dimensions and spatial distribution of pistons are determined only by two characteristic lengths: L_x and L_y. These two characteristic lengths can be determined for any type of shape by its inertia tensor. In this way, an equivalent rectangular geometry can be found for any complex-shaped structure and the number of pistons N determined according to the mode order ($N = m \times n$). Additionally, it is possible to determine the similarity to a rectangular surface by using the inertia tensor and the exact area of the shape.

4.1. Tensor of inertia and characteristic lengths

Consider the 2D inertia tensor I, for a structure with mass $\rho(\mathbf{r_0})$,

$$I = \begin{bmatrix} I_x & -I_{xy} \\ -I_{xy} & I_y \end{bmatrix} = \begin{bmatrix} \iint_S y^2 \rho(\mathbf{r_0}) \mathrm{d}S & -\iint_S xy\rho(\mathbf{r_0}) \mathrm{d}S \\ -\iint_S xy\rho(\mathbf{r_0}) \mathrm{d}S & \iint_S x^2 \rho(\mathbf{r_0}) \mathrm{d}S \end{bmatrix}. \tag{23}$$

The principal axis of inertia comes from the eigenvectors of the inertia tensor. The characteristic lengths embedded within the eigenvalues $\lambda_{1,2}$ are calculated by eigenvalue analysis, expecting exact values if the geometry is known. The components of the inertia tensor for a rectangular surface, normalized by the mass and with respect to the center of inertia, are $I_x = L_x L_y^3/12$ and $I_y = L_x^3 L_y/12$. As for a rectangular surface $S = L_x L_y$, the characteristic lengths and the aspect ratio $\zeta = L_x/L_y$ are given by

$$\begin{aligned} L_{x,y} &= \sqrt{\frac{12\lambda_{1,2}}{S}} \qquad \text{and} \\ \zeta &= \sqrt{\frac{\lambda_1}{\lambda_2}}, \qquad L_x \geq L_y. \end{aligned} \tag{24}$$

4.2. Modal characteristic dimension

In a rectangular structure, the number of lobes are determined by the mode order $N = m \times n$. As all the lobes are considered to be equal, the *equivalent modal radius of radiation* is simply calculated as

$$a_{eq_{mn}} = 1.06 C S_{mn}^{3/4} P_{mn}^{-1/2} \tag{25}$$

where the surface of each lobe for the mode (m,n) is $S_{mn} = L_x L_y / mn$ and the perimeter $P_{mn} = 2(L_x/m + L_y/n)$. To the best of our knowledge, in the literature, there is no reference to equivalent radius to match the radiation of a piston to a plate.

4.3. The distance matrix

Higher order modes can be modeled by placing the center of the pistons in the geometric center of an equally divided rectangle whose dimensions L_x and L_y are given by the inertia tensor in Eq. (24). Thus, the distance between each pair of pistons' centers is determined by the distance matrix [**d**], which coefficients d_{ij} are

$$d_{ij} = \sqrt{\left(\frac{(i-1)L_x}{m}\right)^2 + \left(\frac{(j-1)L_y}{n}\right)^2}, \quad i = 1, 2, \dots, m; \quad j = 1, 2, \dots, n. \tag{26}$$

A larger mode order results in a growing size of the distance matrix since the indices correspond both to the matrix coefficients and to the mode order.

4.4. Mode classification

EPM-RD uses a rectangular model. Assuming that the plate shape is close enough to a rectangle (see Section 4.7.1), we assume that each mode with $N = m \times n$ lobes appears in frequency similarly as it does rectangular plates, i.e.

$$\mathrm{idx}_{mn} = \frac{\zeta^2 m^2 + n^2}{1 + \zeta^2}, \tag{27}$$

where ζ is obtained with Eq. (24). idx_{mn} is a dimensionless frequency giving the order of appearance of modes in rectangular isotropic plates and it is used to assign a modal efficiency to a known resonance frequency. This opens the possibility to estimate an average value of the radiation efficiency (see Eq. (9)).

4.5. Average radiation efficiency of a rectangular plate estimated with the EPM-RD

Due to rectangular structure symmetry, the estimated modal radiation efficiency (refer to Eq. (16)) will contain repeated elements. By counting them, repeated calculations are avoided, speeding up the process. Radiation efficiency can therefore be expressed as a linear combination of the self-efficiencies of the pistons, mutual efficiencies between in- and out-of-phase pairs of pistons, and mutual efficiencies between a pair of pistons with opposite phases. We will refer to pistons with positive velocity as +, and pistons with negative velocity as -. In order to represent a mode with N lobes ($N = N^+ + N^-$), $m \times n$ pistons will be used. The number of radiators in each mode are summarized as follows:

- Self efficiencies : $N = N^+ + N^-$
- Mutual efficiency of positive pairs $\oplus\,\oplus$: $2[{}^{(N^+-1)}C_2] = {}^{(N^+-1)}P_2$
- Mutual efficiency of negative pairs $\ominus\,\ominus$: $2[{}^{(N^--1)}C_2] = {}^{(N^--1)}P_2$
- Mutual efficiency of positive-negative pairs $\oplus\,\ominus$: $2[{}^{(N^--1)(N^+-1)}C_2] = {}^{(N^--1)(N^+-1)}P_2$

where ${}^nC_2$ and ${}^nP_2$ are the combination and permutations of the sources defined as

$${}^nC_k = \frac{n!}{k!(n-k)!},$$
$${}^nP_k = \frac{n!}{(n-k)!}.$$

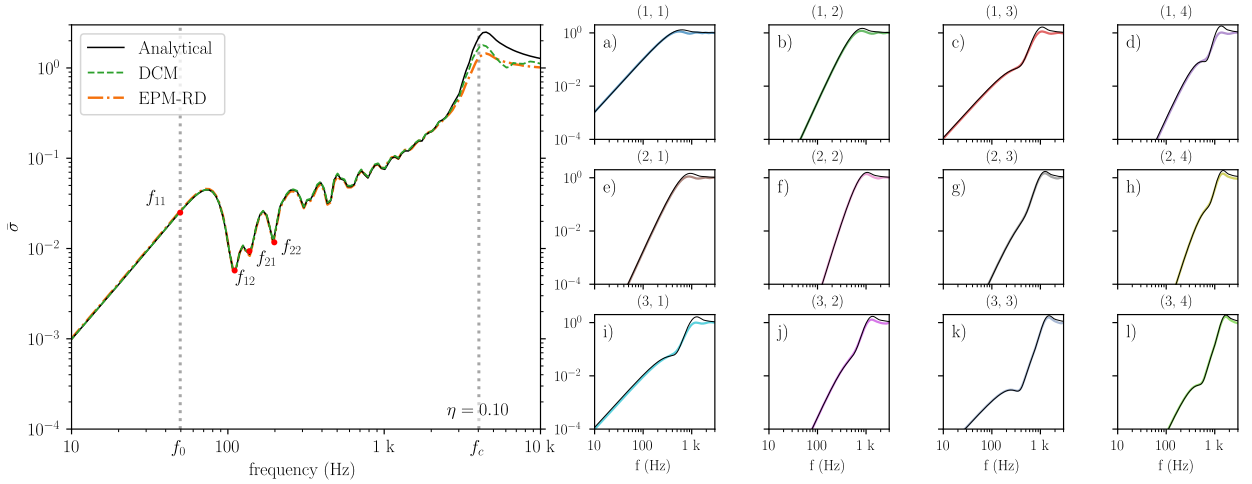

Figure 6: Average radiation efficiency using the first 400 modes. Analytical (solid black line ——), semi-analytical Hashimoto's direct calculation method (DCM [29], dashed green line - - -) and simplified equivalent piston model (EPM-RD, dash-dotted line - · -). The right side shows some modal efficiencies: analytical (black solid lines) and using the EPM-RD (colored lines).

The radiation efficiency can be expressed simply by a sum of self and mutual efficiencies as

$$\sigma_{mn} = \sigma_p(a) + \frac{1}{N}\left(\underbrace{\sum_{i=1}^{(N^+-1)P_2} \sigma_{2p}(a, d_i)}_{\oplus\oplus} + \underbrace{\sum_{i=1}^{(N^--1)P_2} \sigma_{2p}(a, d_i)}_{\ominus\ominus} - \underbrace{\sum_{i=1}^{(N^+-1)(N^--1)P_2} 2\sigma_{2p}(a, d_i)}_{\oplus\ominus} \right). \tag{28}$$

The plus sign before the mutual efficiency comes from the pistons vibrating in-phase, either positive or negative, which increases radiation efficiency. On the other hand, the minus sign indicates that pistons are in vibrating in anti-phase and decreasing radiation efficiency.

Consider the aluminum rectangular simply supported plate with dimensions of $0.6 \times 0.5 \times 3^{-3}$ m^3 (volumetric density $\rho = 2700$ kg.m^{-3} and Poisson coefficient $\nu = 0.3$) studied by Wallace [14], Arenas [25] and Xie et al. [13]. Figure 6 shows the estimated average radiation using the EPM-RD with two characteristic lengths given by the inertia tensor (see Eq. (24)). We observe a very good agreement, on a wide frequency range up to the coincidence frequency, compared to the analytical solution [4, 13] and the discrete calculation method (DCM) [29]. The piston approach allows us to examine the modal efficiency deeply, opening the possibility to formulate simple equations that can be derived directly from Eq. (28) and which are summarized in Table 2.

The low-frequency pattern of each mode is determined by the remaining radiators, just as it is with corner and edge modes. The last slope is proportional to $2(m + n - 1)$ power just below the coincidence frequency, also appointed by Honda et al. [5] for circular plates. A slope change requires at least three pistons in the rectangular case (see Fig. 6c for example) and two or more radiators of different sizes in more complex structures (see Figs. 5, 7 and 8). If more than three pistons are considered, the transition between slopes is a bit more complex to analyze; note that Eq. (18) has a $\mathrm{sinc}(x)$ function, which eliminates the mutual effects approximately when $kd_{ij} = \pi$. Take a look modes (3,1) or (1,3) in a rectangular plate; whenever there are at least three radiators present, two must be in phase, and the third in phase opposition. A transition occurs at the closest distance between two in-phase pistons, pistons one and three in this example. As such, this is true for any mode, however, since other radiators may be contributing to the radiation at this frequency, we cannot state whether this is an upper or lower bound. All of these features are precisely captured by the equivalent piston model.

As pistons are arranged in a symmetric array, we can count the pairs of pistons that are repeated and calculate the mutual efficiency only once (Eq. (28) instead of Eq. (16)). Additionally, equal-sized pistons can be used to model each mode lobe (Eq. (19) instead of Eq. (18)). As a result of both simplifications, the computation time is reduced.

Table 2
Modal radiation efficiency. The low-limit radiation corresponds to edge and corner radiation. Just below the coincidence frequency, the radiation is proportional to the $2(m+n-1)$ power. The transition of slopes occurs near kd, where d is the distance of the nearest pair of in-phase pistons in the array.

Mode	General Equation (28)	ka ≪ 1	$k < k_p$	Transition	Fig. 6
1,1	σ_p	$(ka)^2$	-	-	a
1,2	$\sigma_p - \sigma_{2p}(d_y)$	$(ka)^4$	-	-	b
2,2	$\sigma_p - \sigma_{2p}(d_y) - \sigma_{2p}(d_x) + \sigma_{2p}(d_{xy})$	$(ka)^6$	-	-	f
1,3	$\sigma_p - \frac{4}{3}\sigma_{2p}(d_y) + \frac{2}{3}\sigma_{2p}(2d_y)$	$(ka)^2$	$(ka)^6$	$\sim \pi/2d_y$	c
2,3	$\sigma_p - \frac{4}{3}\sigma_{2p}(d_y) - \sigma_{2p}(d_x) + \frac{4}{3}\sigma_{2p}(d_{xy}) + \ldots$	$(ka)^4$	$(ka)^8$	$\sim \pi/d_{xy}$	g
1,4	$\sigma_p - \frac{3}{2}\sigma_{2p}(d_y) + \sigma_{2p}(2d_y) - \frac{1}{2}\sigma_{2p}(3d_y)$	$(ka)^4$	$(ka)^8$	$\sim \pi/2d_y$	d
2,4	$\sigma_p - \frac{3}{2}\sigma_{2p}(d_y) - \sigma_{2p}(d_x) + \frac{3}{2}\sigma_{2p}(d_{xy}) + \ldots$	$(ka)^6$	$(ka)^{10}$	$\sim \pi/d_{xy}$	h

In the next section, we will discuss some of the effects that may occur in modes efficiency that are not present in rectangular plates. In particular, residual monopoles and dipoles may be present at low frequencies in structures with reduced symmetry.

4.6. Limitations of the EPM-RD and dissymmetry's effects

As stated earlier, the highly symmetrical rectangular model provides many advantages for estimating radiation. However, in less simple structures, this symmetry may not be present. By breaking the symmetry, the distribution of the lobes, their sizes, and their mean flux change, and therefore how the structure radiates sound changes. Therefore, residual radiators may be present and the residual monopole is the primary residual radiator to appear, although higher-order residual radiators may also be present.

4.6.1. Residual monopole

Figure 7 shows the second mode of a dissymmetric-shaped plate. Due to dissymmetry, the radiation exhibits a residual monopole at low frequencies, which can be modeled by identifying the nodal lines and volume velocity for each lobe. By doing so, a precise distribution of pistons can match the modal radiation. This is illustrated in Fig. 7a, using Eq. (14). We can also observe the same effect on the efficiency plot (with Eq. (15)) if we take the same amplitude velocity for both pistons and change only their sizes (Fig. 7b).

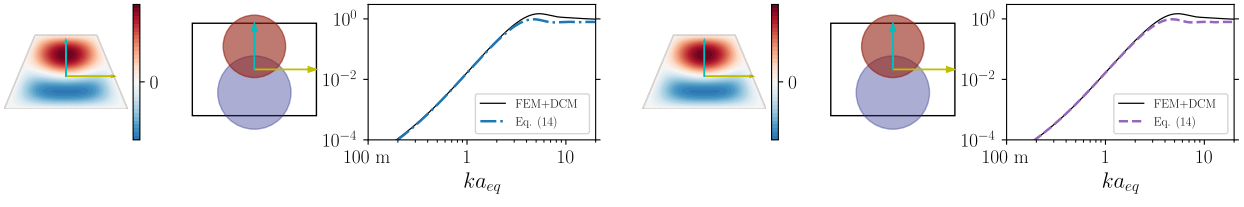

(a) (b)

Figure 7: An dissymmetrical shape creates a residual monopole for even modes. FEM+DCM [29] (solid black lines ——) compared to a) pistons with different volume velocities (blue dashed lines - - -) and b) different-sized pistons with equal velocity amplitudes (purple dashed lines - - -).

As residual monopoles are fundamentally linked to residual flux, the same pattern can also be reproduced by a pair of pistons of the same size vibrating with different amplitudes, as seen in Fig. 8b. The use of identical pistons simplifies the formulation and speeds up the calculation of the radiation, while keeping similar accuracy.

Higher-order even modes may also exhibit similar residual monopolar behavior. Consider the mode four of a parallelogram plate (Fig. 9). This mode typically is classified as a quadrupole in rectangular plates, i.e. the mode

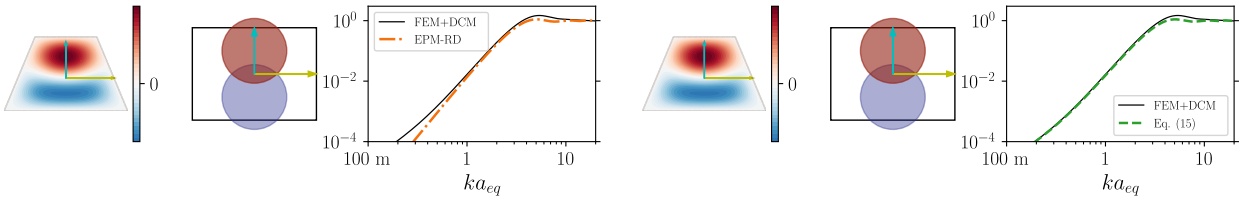

Figure 8: Simplified method to include residual monopole effects at low frequencies. FEM+DCM [29] (solid black lines ——) compared to a) EPM-RD (orange dash-dotted lines - · -) and b) equal-sized pistons with different velocity amplitudes (green dashes lines - - -).

(2,2). However, in this case the total volume velocity is different from zero. Once again, the low-frequency trend can be recovered by integrating the mode on the piston's surface and determining the difference in piston velocity.

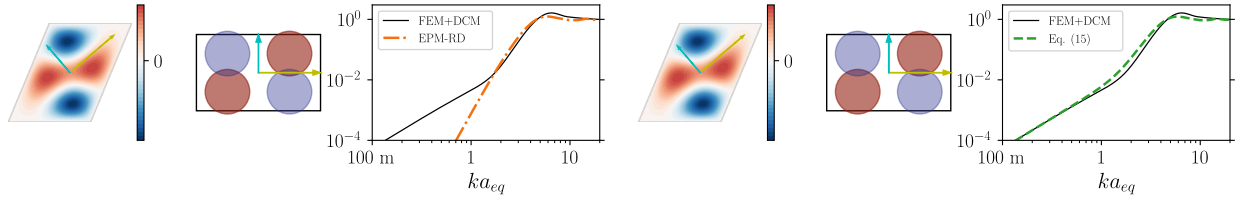

Figure 9: Residual monopole in a four-lobe mode. FEM+DCM [29] (solid black lines ——) compared to a) EPM-RD (orange dash-dotted lines - · -) and b) equal-sized pistons with different velocity amplitudes (green dashed lines - - -).

4.6.2. Residual dipole

In the same lane, any shape with less regularity than a rectangle may also possess residual higher order residual radiators, as seen in Fig. 10. A symmetrical trapezoidal shape, for instance, exhibits a residual dipole, as opposed to the perfect quadrupole of a rectangular shape (mode (2,2)). In this case, the center of mass of positive velocities is located at a different location from the center of mass of negative velocities.

Figure 10a shows the EPM-RD calculation of mode four on a trapezoidal plate compared to a discrete calculation. As a result of the mode symmetry, the total flux is zero, and the slope (solid black line) of the efficiency changes from dipolar to quadrupolar slope before the coincidence frequency. EPM (dashed orange line) only captures quadrupolar behavior, whose slope lies between dipolar and quadrupolar slopes.

In order to obtain the exact trend, one can alter the pistons' positions to create a dipole by breaking the symmetry (Fig. 10d). Additionally, it should be noted that in the first case (Fig. 10a), the two pistons are located too far apart to predict accurately the quadrupolar behavior. This effect is captured by reducing distance between pistons, as illustrated in Fig. 10b.

A similar behavior might be observed in higher order modes with specific radiation patterns (octupole, etc). Generally, these small errors will not have a significant effect on the average efficiency. However, pistons can also be adjusted in the same way to smooth out these deviations.

4.7. Robustness of the EPM-RD model concerning the plate geometry

The presented model assigns a radiation curve to a particular resonance frequency. This assignment is based on the sorted order of resonance frequencies in a rectangular plate. With Eqs. (24) and (27) we can determine the sorted order of resonance frequencies of the equivalent rectangular plate. Since the EPM-RD only considers a regular paving of the pistons, the ability to deal with different plate shapes relates to how distant these plates are from rectangular geometries. In order to estimate the robustness of the EPM-RD model, the ratio of its actual surface to the surface $S = L_x L_y$ obtained from the inertia tensor can be used to calculate the distance between a rectangular shape and

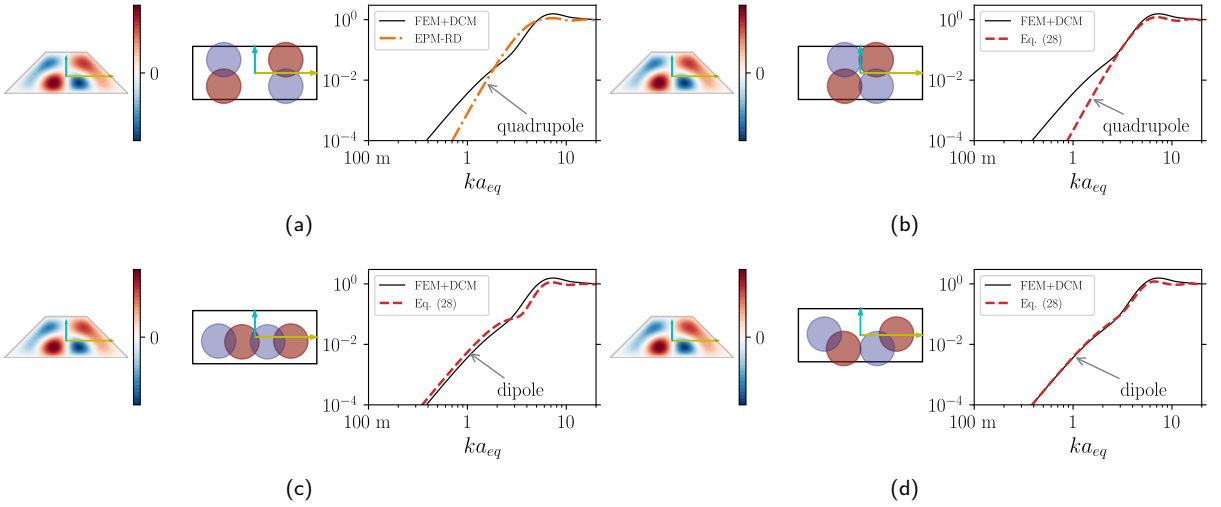

Figure 10: Residual dipole in a four-lobe mode. FEM+DCM [29] (solid black lines ——) of mode four compared to pistons with a) EPM-RD (orange dash-dotted lines - · - ·) and b,c,d) Different pistons' positions and their effects on the modal radiation (red dashed lines - - -) using the EPM.

the considered shape. Figure 11 illustrates the sorted deviation for several shapes presented in the present paper. The smaller the difference between the structure surface and the equivalent rectangle, the better the EPM-RD should predict the radiation.

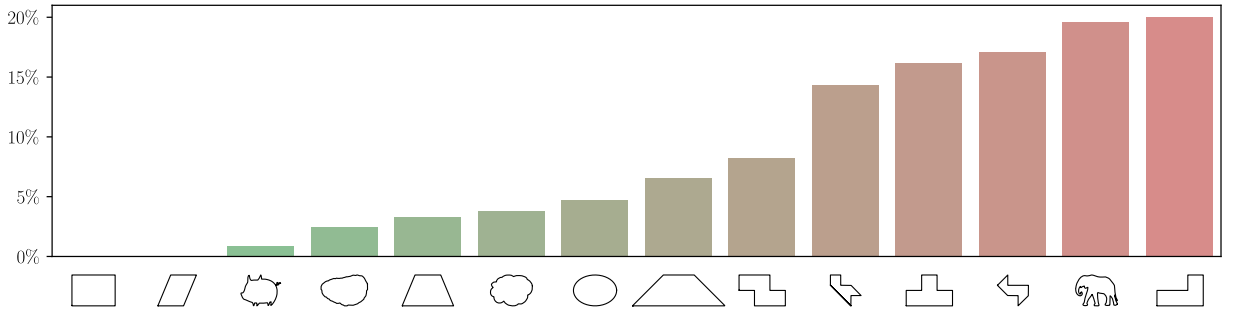

Figure 11: Relative surface deviation from the equivalent rectangular area $S = L_x L_y$. Comparing the geometry's area with that calculated with the inertia tensor can be helpful in estimating the dissimilarity with the rectangular shape.

4.7.1. Plates with slight deviations from rectangular shapes

Figure 12 illustrates the modal radiation calculated by FEM-DCM for four plate shapes "close" to a rectangular surface. According to the simplified equivalent piston model (EPM-RD), the modal radiation estimates are in good agreement with the numerical results. For the first mode, all cases agree fairly well, even when the boundaries are not smooth (see shapes c) and d) in Fig. 12). As for the second mode, the low frequency radiation is slightly underestimated for shapes b) and d) due to their greater dissymmetry. The radiation is not that of a pure dipole and there is a residual monopole which could be better matched as indicated in 4.6.1.

In Fig. 13, the average radiation efficiency and mean power are compared with the DCM calculation for the four plates previously shown in Fig. 12. Even though the damping factor is very low, $\eta = 0.01$, rather than the more standard $\eta = 0.1$ found in the literature [13, 25], there is good agreement between the radiation resistance matrix formulation and the piston approach. This value was chosen to highlight the differences between EPM-RD and DCM models.

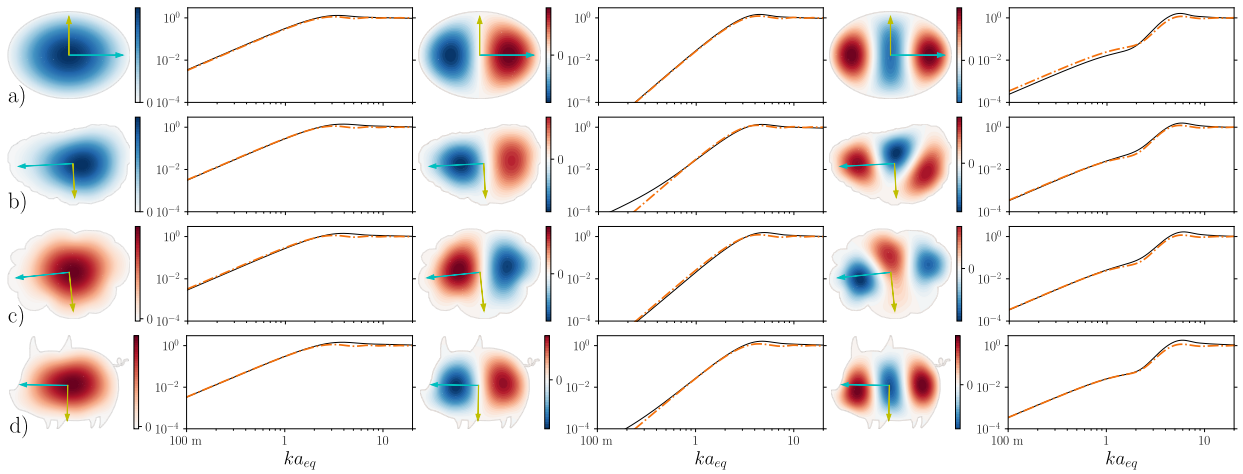

Figure 12: First mode shapes of several plates computed with FEM [53], with arrows showing characteristic directions and lengths based on eigenanalysis of the inertia tensor. The characteristic lengths can be used to estimate the equivalent radius of radiation and the locations of the pistons. Each mode shape is associated with a modal efficiency calculated using FEM+DCM [29] (solid black lines ——) and compared to the EPM-RD (orange dash-dotted lines - · -).

Furthermore, this difference gets accentuated in the radiation efficiency, but not that much in the mean power radiated by the structure, with remarkable differences only at some frequencies. Since we are using finite element analysis to calculate resonance frequencies, the source of error lies in the classification of modes rather than in the estimated modal radiation. For instance, a mode that radiates at low frequencies effectively as a monopole, i.e. mode (3,1), (5,3), etc., can be confused with a mode that radiates in the low frequency as a dipole, such as modes (4,1), (5,2), and so on. The mismatch can lead to significant increase or decrease in the average radiation efficiency at resonance frequencies, but less pronounced differences on the radiated power.

4.7.2. Plates with significant deviation from rectangular shapes

Consider the plate shown in Fig. 14. Compared to the previous shapes, this plate has a less simple distribution of mass. This results in an irregular distribution of modal lines due to the non-orthogonal paving of the modes, which differs greatly from the approach taken in the EPM-RD, resulting in modes that cannot found an equivalent in rectangular arrays. Furthermore, using the sorted order of the modes as in the rectangular case may not be the best strategy. Even so, when pistons are placed at the mode peaks and using the same equivalent modal radiation radius as before, the EPM can still approximate these modes, particularly mode four (Fig. 14b), closer to a parallelogram or even to the "Z" shape in the tetris example (Fig. 5). It is then necessary to provide the EPM with a model for positioning radiators optimally and automatically in order to better estimate more complex-shaped plates, where the rectangular model is insufficient.

5. Discussion

Our proposed EPM allows us to estimate the modal efficiency of complex structures and the EPM-RD the average power and efficiency. It is wordy to emphasize that piston models have some advantages, including the ability to calculate average radiation and mean power quickly, as well as the possibility to derive analogous analytical formulations of modal efficiencies for complex shapes. This is especially useful for analyzing the transitions and waviness present in some modal efficiencies; deconstructing the radiation efficiency allows us to examine this kind of behavior in depth.

As shown in Eqs. (4) and (5), to calculate the average radiation with a discrete numerical approach, the ARM must be calculated for each frequency for each mode, a procedure that may take a long time, but is still faster than using finite elements or boundary elements. Because the size of an ARM is determined by the square of the number of discrete elements, it is important to consider the size of the computer's RAM as well. This may also contribute to the under-utilization of modal approaches for studying structure average radiation. By removing these time and

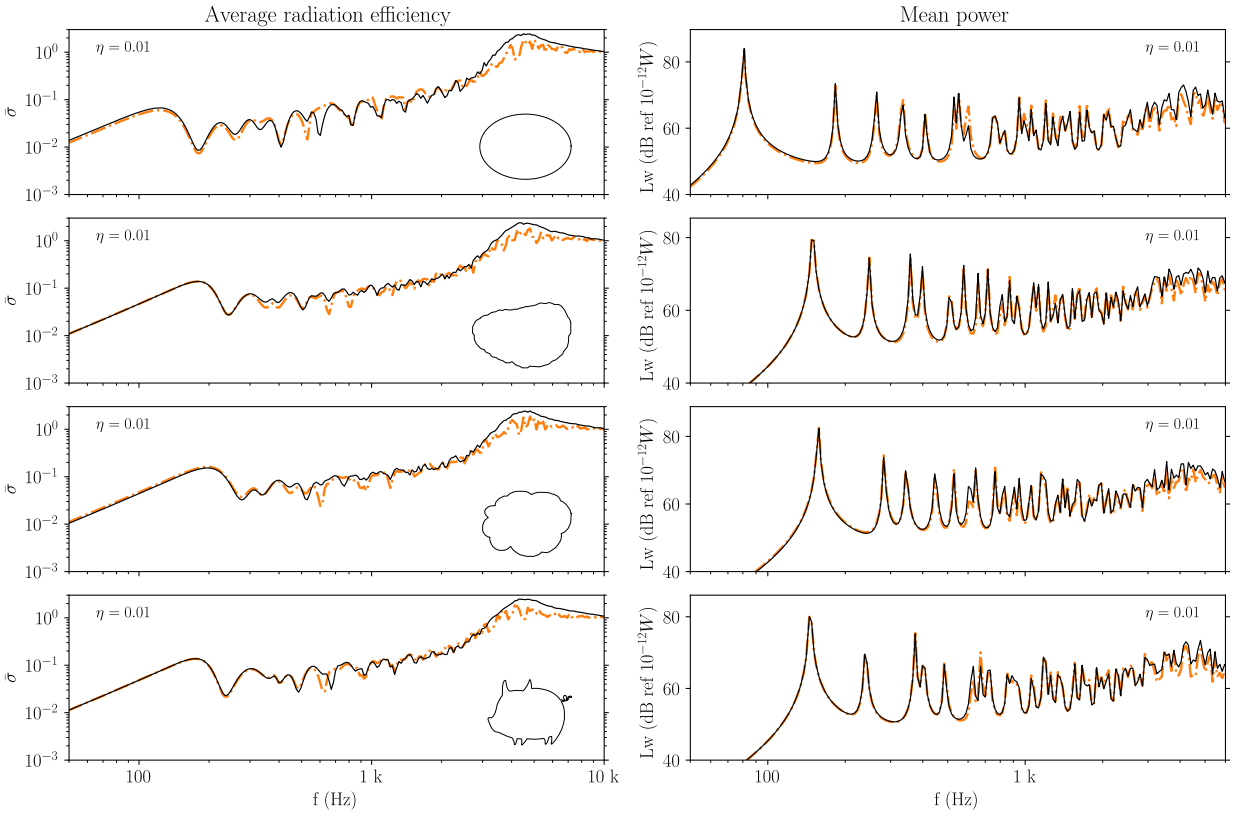

Figure 13: Average radiation of four plates with equal surfaces and constant damping $\eta = 0.01$. The reference value given by FEM+DCM (solid black lines ——) is compared to the piston approach (orange dash-dotted lines - · -).

computational barriers, EPM and EPM-RD can become valuable estimation tools since, for instance, calculating the average radiation efficiency for a given plate geometry takes only a few seconds with the EPM-RD.

The method could be improved in some ways, such as determining automatically the location of pistons in the EPM to treat any shape, as shown in Fig. 14. It would also be useful to include non-uniform velocity profiles (see [54, 55, 56, 51]), in order to mimic the smooth transition between lobes and reduce the gap above the critical frequency.

By comparing the plate shapes with their equivalent rectangular surfaces, we can classify them according to the degree of similarity to rectangles. As a result, we can determine the precision of our approach and whether or not it is convenient to use the EPM-RD. There is still a large gap in determining eigenfrequencies without using finite element analysis. The rectangular plate model (see Eq. (27)) may be adequate for classifying modes, but it may fail to predict eigenfrequencies. Such improvements can transform this method into a purely geometrical method for estimating the radiation of complex-shaped plates.

6. Conclusion

We present a general method for estimating modal radiation efficiencies of complex-shaped plates based on vibrating pistons (EPM). Equivalent-sized pistons replicate the vibrations of each lobe within the mode shapes, whose dimensions are determined by the geometrical information contained within the structure. Various scenarios illustrate how to match modal efficiencies based on piston size and volume velocity. As symmetry starts to break, general effects can be spotted; such as non-null-flux "even" modes radiating as monopoles as a result of their uncancelled volume velocity. Even modes in slightly asymmetrical shapes may present higher-order residual radiators, which are easily modeled by adjusting the piston positions. Through Tetris-shaped plates, we illustrate how different piston positioning affects the modal radiation. The EPM provides analytical formulations that are not readily available for structures with complex shapes.

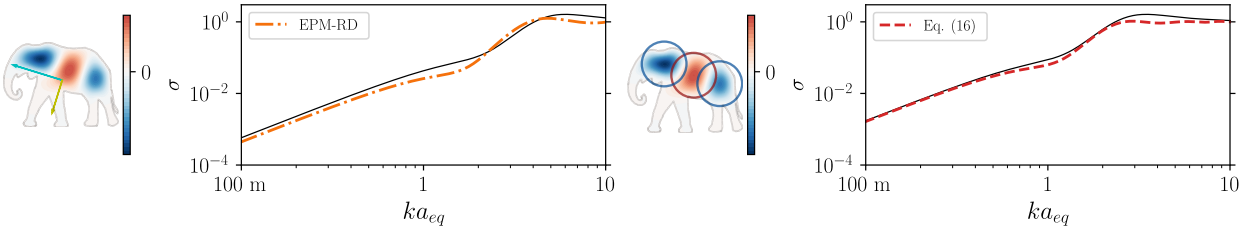

(a) Mode 3

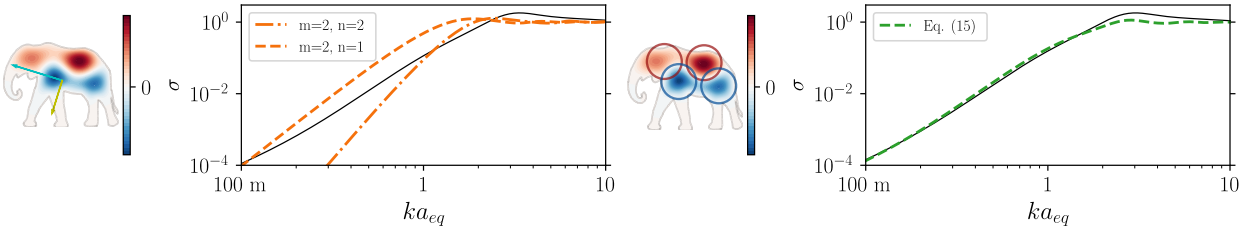

(b) Mode 4

Figure 14: EPM-RD cannot be used directly in this case because of the irregular mass distribution in the plate. Comparison of FEM+DCM (solid black lines ——) calculations with EPM-RD (orange dashed-dotted lines - · - ·) and with pistons whose positions are adapted manually to match properly the mode shape (red and green dashed lines).

Average values of the mean-square velocity, power and radiation efficiency are found by averaging over all possible excitation positions. This formulation implies the Equipartition Theorem and consequently, since all modes are equally excited, there is no acoustic coupling between modes when calculating the average radiated power. By using this average formulation, we can separate radiation from excitation, which is useful for finding global indicators. It helps also, as a side note, to explain why *one can actually hear the shape of a drum* even for isospectral geometries, i.e. in vibration argot, structures with the same average mean-square velocity.

We also derive a specific version (EPM-RD) for geometries close to rectangles. We use finite element analysis to calculate the eigenfrequencies, a rectangular plate model to correlate each frequency with the estimated modal efficiency and the average definition to find the global parameters of acoustic radiation. Using the inertia tensor, it is possible to determine two characteristic lengths for setting the pistons' size and position in a rectangular array. The radiation of a rectangular plate can be approximated very precisely using this formulation, for a far less expensive computation than an analytical solution. The simplified method SPEM is examined on plates of various geometries, in order to illustrate its limitations, such as missing residual radiators or some mismatches when a modal efficiency does not correspond to a frequency mode. Nonetheless, if the shape is in some way "similar" to a rectangle, EPM-RD can be used efficiently to estimate the acoustic radiated power and efficiency.

The rectangular model provides a simple and complete method for evaluating the acoustic radiation of plates. Aside from this possibility, as we have shown, pistons can be combined in other ways for better estimating the efficiency, which is applicable to a wider range of geometries. The versatility of expressing radiated efficiency with pistons of different sizes, amplitudes, and phases, as well as the simplicity of the formulation, suggest great potential for equivalent piston-based models. Additionally, this work may serve to predict the radiation of localized modes in plates or membranes [48]. A further perspective of this work is to include in the model a method for estimating eigenfrequencies solely based on the geometry and material of the structure, without any dynamical analysis.

References

[1] Lord Rayleigh. *The theory of sound*, volume 2. Dover Publications, New York, 2 edition, 1945.

[2] Gideon Maidanik. Response of Ribbed Panels to Reverberant Acoustic Fields. 1962. URL https://asa.scitation.org/doi/10.1121/1.1918200.

[3] Arthur W. Leissa. *Vibration of Plates*. Phio State Univerity, 1969.

[4] C. E. Wallace. Radiation Resistance of a Rectangular Panel. *The Journal of the Acoustical Society of America*, 51(3B):946–952, March 1972. ISSN 0001-4966. doi: 10.1121/1.1912943. URL https://asa.scitation.org/doi/10.1121/1.1912943. Publisher: Acoustical Society of America.

[5] Y. Honda, H. Matsuhisa, and S. Sato. Radiation efficiency of a baffled circular plate in flexural vibration. *Journal of Sound and Vibration*, 88 (4):437–446, June 1983. ISSN 0022-460X. doi: 10.1016/0022-460X(83)90647-8. URL https://www.sciencedirect.com/science/article/pii/0022460X83906478.

[6] Wojciech P. Rdzanek. The acoustic power of a vibrating clamped circular plate revisited in the wide low frequency range using expansion into the radial polynomials. *The Journal of the Acoustical Society of America*, 139(6):3199, June 2016. ISSN 0001-4966. doi: 10.1121/1.4954265. URL https://asa.scitation.org/doi/abs/10.1121/1.4954265. Publisher: Acoustical Society of America.

[7] Noureddine Atalla, Jean Nicolas, and Carol Gauthier. Acoustic radiation of an unbaffled vibrating plate with general elastic boundary conditions. *The Journal of the Acoustical Society of America*, 99(3):1484–1494, March 1996. ISSN 0001-4966. doi: 10.1121/1.414727. URL https://asa.scitation.org/doi/10.1121/1.414727. Publisher: Acoustical Society of America.

[8] B. Laulagnet. Sound radiation by a simply supported unbaffled plate. *The Journal of the Acoustical Society of America*, 103(5):2451–2462, May 1998. ISSN 0001-4966. doi: 10.1121/1.422765. URL https://asa.scitation.org/doi/10.1121/1.422765. Publisher: Acoustical Society of America.

[9] A. Putra and D. J. Thompson. Sound radiation from rectangular baffled and unbaffled plates. *Applied Acoustics*, 71(12):1113–1125, December 2010. ISSN 0003-682X. doi: 10.1016/j.apacoust.2010.06.009. URL https://www.sciencedirect.com/science/article/pii/S0003682X10001490.

[10] R. F. Keltie and H. Peng. The Effects of Modal Coupling on the Acoustic Power Radiation From Panels. *Journal of Vibration, Acoustics, Stress, and Reliability in Design*, 109(1):48–54, January 1987. ISSN 0739-3717. doi: 10.1115/1.3269394. URL https://doi.org/10.1115/1.3269394.

[11] E. J. Skudrzyk. *Simple and Complex Vibratory Systems*. Pennsylvania State University Press,, 1968.

[12] L. Cremer and M. Heckl. *Structure-Borne Sound*. Springer, Berlin, Heidelberg, 2 edition, 1988. ISBN 3-540-18241-5. URL https://doi.org/10.1007/978-3-662-10121-6.

[13] G. Xie, D. J. Thompson, and C. J. C. Jones. The radiation efficiency of baffled plates and strips. *Journal of Sound and Vibration*, 280 (1):181–209, February 2005. ISSN 0022-460X. doi: 10.1016/j.jsv.2003.12.025. URL https://www.sciencedirect.com/science/article/pii/S0022460X0400063X.

[14] C. E. Wallace. Radiation Resistance of a Baffled Beam. *The Journal of the Acoustical Society of America*, 51(3B):936–945, March 1972. ISSN 0001-4966. doi: 10.1121/1.1912942. URL https://asa.scitation.org/doi/10.1121/1.1912942. Publisher: Acoustical Society of America.

[15] Earl G. Williams. A series expansion of the acoustic power radiated from planar sources. *The Journal of the Acoustical Society of America*, 73(5):1520–1524, May 1983. ISSN 0001-4966. doi: 10.1121/1.389412. URL https://asa.scitation.org/doi/10.1121/1.389412. Publisher: Acoustical Society of America.

[16] W. L. Li. AN ANALYTICAL SOLUTION FOR THE SELF- AND MUTUAL RADIATION RESISTANCES OF A RECTANGULAR PLATE. *Journal of Sound and Vibration*, 245(1):1–16, August 2001. ISSN 0022-460X. doi: 10.1006/jsvi.2000.3552. URL https://www.sciencedirect.com/science/article/pii/S0022460X00935521.

[17] Laurent Bouchet. *Calcul du rayonnement acoustique de structures à partir de données vibratoires par une méthode de sphère équivalente*. PhD thesis, ECL - INSA - UCBL, 1996.

[18] Haijun Wu, Weikang Jiang, Yilin Zhang, and Wenbo Lu. A method to compute the radiated sound power based on mapped acoustic radiation modes. *The Journal of the Acoustical Society of America*, 135(2):679–692, February 2014. ISSN 0001-4966. doi: 10.1121/1.4861242. URL https://asa.scitation.org/doi/10.1121/1.4861242. Publisher: Acoustical Society of America.

[19] Carlos García A., Nicolas Dauchez, and Gautier Lefebvre. Radiation efficiency of a distribution of baffled pistons with arbitrary phases. *The Journal of the Acoustical Society of America*, 152(2):1135–1145, August 2022. ISSN 0001-4966. doi: 10.1121/10.0013569. URL https://asa.scitation.org/doi/10.1121/10.0013569. Publisher: Acoustical Society of America.

[20] M. C. Gomperts. Sound Radiation from Baffled, Thin, Rectangular Plates. *Acta Acustica united with Acustica*, 37(2):93–102, March 1977.

[21] C. Bouwkamp. Theoretical and numerical treatment of diffraction through a circular aperture. *IEEE Transactions on Antennas and Propagation*, 18(2):152–176, March 1970. ISSN 1558-2221. doi: 10.1109/TAP.1970.1139646. Conference Name: IEEE Transactions on Antennas and Propagation.

[22] R. J. Donato. Direct derivation of radiation resistance of a vibrating panel. *Journal of Sound and Vibration*, 28(1):87–92, May 1973. ISSN 0022-460X. doi: 10.1016/S0022-460X(73)80019-7. URL https://www.sciencedirect.com/science/article/pii/S0022460X73800197.

[23] C. L. Dym. A more direct derivation of the radiation resistance of a panel. *Journal of Sound and Vibration*, 32(2):279–282, January 1974. ISSN 0022-460X. doi: 10.1016/S0022-460X(74)80170-7. URL https://www.sciencedirect.com/science/article/pii/S0022460X74801707.

[24] Jorge P. Arenas. On the Sound Radiation From a Circular Hatchway. *International Journal of Occupational Safety and Ergonomics*, 15(4): 401–407, January 2009. ISSN 1080-3548. doi: 10.1080/10803548.2009.11076819. URL https://doi.org/10.1080/10803548.2009.11076819. Publisher: Taylor & Francis _eprint: https://doi.org/10.1080/10803548.2009.11076819.

[25] Jorge P. Arenas. Numerical computation of the sound radiation from a planar baffled vibrating surface. *J. Comp. Acous.*, 16(03):321–341, September 2008. ISSN 0218-396X. doi: 10.1142/S0218396X08003671. URL https://www.worldscientific.com/doi/abs/10.1142/S0218396X08003671. Publisher: World Scientific Publishing Co.

[26] Frank Fahy. Sound and Structural Vibration - 2nd Edition, 2007. URL https://www.elsevier.com/books/sound-and-structural-vibration/fahy/978-0-12-373633-8.

[27] Scott D. Snyder and Nobuo Tanaka. Calculating total acoustic power output using modal radiation efficiencies. *The Journal of the Acoustical Society of America*, 97(3):1702–1709, March 1995. ISSN 0001-4966. doi: 10.1121/1.412048. URL https://asa.scitation.org/doi/10.1121/1.412048. Publisher: Acoustical Society of America.

[28] Arthur P. Berkhoff. Sensor scheme design for active structural acoustic control. *The Journal of the Acoustical Society of America*, 108(3):1037–1045, September 2000. ISSN 0001-4966. doi: 10.1121/1.1286514. URL https://asa.scitation.org/doi/10.1121/1.1286514. Publisher: Acoustical Society of America.

[29] N Hashimoto. Measurement of sound radiation efficiency by the discrete calculation method. *Applied Acoustics*, 62(4):429–446, April 2001. ISSN 0003-682X. doi: 10.1016/S0003-682X(00)00025-6. URL http://www.sciencedirect.com/science/article/pii/S0003682X00000256. Number: 4.

[30] J. S. Tao, G. R. Liu, and K. Y. Lam. Sound radiation of a thin infinite plate in light and heavy fluids subject to multi-point excitation. *Applied Acoustics*, 62(5):573–587, May 2001. ISSN 0003-682X. doi: 10.1016/S0003-682X(00)00047-5. URL https://www.sciencedirect.com/science/article/pii/S0003682X00000475.

[31] P. M. Morse and K. U. Ingard. *Theoretical acoustics*. McGraw-Hill, New York, 1968.

[32] K. Gösele. Schallabstrahlung von Platten, die zu Biegeschwingungen angeregt sind. *Acta Acustica united with Acustica*, 3(4):243–248, January 1953.

[33] Earl G. Williams. *FOURIER ACOUSTICS Sound Radiation and Nearfield Acoustical Holography*. 1999.

[34] Azma Putra. *Sound radiation from perforated plates*. phd, University of Southampton, June 2008. URL https://eprints.soton.ac.uk/63161/.

[35] Yiwei Kou, Bilong Liu, and Jing Tian. Radiation efficiency of damped plates. *The Journal of the Acoustical Society of America*, 137(2):1032–1035, February 2015. ISSN 0001-4966. doi: 10.1121/1.4906186. URL https://asa.scitation.org/doi/10.1121/1.4906186. Publisher: Acoustical Society of America.

[36] John L. Davy. The forced radiation efficiency of finite size flat panels that are excited by incident sound. *The Journal of the Acoustical Society of America*, 126(2):694–702, August 2009. ISSN 0001-4966. doi: 10.1121/1.3158820. URL https://asa.scitation.org/doi/10.1121/1.3158820. Publisher: Acoustical Society of America.

[37] Ronald M. Aarts and Augustus J. E. M. Janssen. Sound radiation quantities arising from a resilient circular radiator. *The Journal of the Acoustical Society of America*, 126(4):1776–1787, October 2009. ISSN 0001-4966. doi: 10.1121/1.3206580. URL https://asa.scitation.org/doi/full/10.1121/1.3206580.

[38] Martin Greenspan. Piston radiator: Some extensions of the theory. *The Journal of the Acoustical Society of America*, 65(3):608–621, March 1979. ISSN 0001-4966. doi: 10.1121/1.382496. URL https://asa.scitation.org/doi/10.1121/1.382496. Publisher: Acoustical Society of America.

[39] F. G. Leppington, E. G. Broadent, and K. J. Heron. The acoustic radiation efficiency of rectangular panels. *Proceedings of the Royal Society of London. A. Mathematical and Physical Sciences*, August 1982. doi: 10.1098/rspa.1982.0100. URL https://royalsocietypublishing.org/doi/abs/10.1098/rspa.1982.0100. Publisher: The Royal Society London.

[40] D. Edwins and S. S. Rao. *Encyclopedia of vibration*. 2001.

[41] C. Lesueur. *Rayonnement acoustique des structures: vibroacoustique, interactions fluide-structure [Acoustic radiation of structures: vibroacoustics, fluid-structure interactions]*. Collection de la Direction des études et recherches d'Electricité de France. Eyrolles, 1988. ISBN 978-2-212-01613-0.

[42] Jorge Arenas and Malcolm Crocker. Sound Radiation Efficiency of a Baffled Rectangular Plate Excited by Harmonic Point Forces Using its Surface Resistance Matrix. *IJAV*, 7(4), 2002. ISSN 24151408. doi: 10.20855/ijav.2002.7.4120. URL http://iiav.org/ijav/content/volumes/7_2002_1380281272264886/vol_4/333_firstpage_486791287053352.pdf. Number: 4.

[43] Lord Rayleigh. LIII. Remarks upon the law of complete radiation. *The London, Edinburgh, and Dublin Philosophical Magazine and Journal of Science*, 49(301):539–540, June 1900. ISSN 1941-5982. doi: 10.1080/14786440009463878. URL https://doi.org/10.1080/14786440009463878. Publisher: Taylor & Francis _eprint: https://doi.org/10.1080/14786440009463878.

[44] Mark Kac. Can One Hear the Shape of a Drum? *The American Mathematical Monthly*, 73(4):1–23, 1966. ISSN 0002-9890. doi: 10.2307/2313748. URL https://www.jstor.org/stable/2313748. Publisher: Mathematical Association of America.

[45] Carolyn Gordon, David Webb, and Scott Wolpert. One Cannot Hear the Shape of a Drum. *Bull Am Math Soc*, 27, July 1992. doi: 10.1090/S0273-0979-1992-00289-6.

[46] C. Gordon, D. Webb, and S. Wolpert. Isospectral plane domains and surfaces via Riemannian orbifolds. *Invent Math*, 110(1):1–22, December 1992. ISSN 1432-1297. doi: 10.1007/BF01231320. URL https://doi.org/10.1007/BF01231320.

[47] S. Sridhar and A. Kudrolli. Experiments on not "hearing the shape" of drums. *Phys. Rev. Lett.*, 72(14):2175–2178, April 1994. doi: 10.1103/PhysRevLett.72.2175. URL https://link.aps.org/doi/10.1103/PhysRevLett.72.2175. Publisher: American Physical Society.

[48] Carlos García A., Nicolas Dauchez, Yorick Buot de l'Epine, and Gautier Lefebvre. Localized modes prediction in a membrane with non-uniform tension from the quasi-static measurement of its localization landscape. *Journal of Sound and Vibration*, 511:116272, October 2021. ISSN 0022-460X. doi: 10.1016/j.jsv.2021.116272. URL https://www.sciencedirect.com/science/article/pii/S0022460X21003436.

[49] Dongjoon Kim and No-Cheol Park. Calculation and reduction of sound radiation from a thin plate structure excited by complex inputs. *Journal of Sound and Vibration*, 484:115517, October 2020. ISSN 0022-460X. doi: 10.1016/j.jsv.2020.115517. URL https://www.sciencedirect.com/science/article/pii/S0022460X20303497.

[50] Kenneth A. Cunefare, M. Noelle Currey, M. E. Johnson, and S. J. Elliott. The radiation efficiency grouping of free-space acoustic radiation modes. *The Journal of the Acoustical Society of America*, 109(1):203–215, January 2001. ISSN 0001-4966. doi: 10.1121/1.1323236. URL https://asa.scitation.org/doi/10.1121/1.1323236. Publisher: Acoustical Society of America.

[51] Leo L. Beranek and Tim J. Mellow. *Acoustics Sound Fields, Transducers and Vibration*. Academic Press, second edition edition, 2019. ISBN 978-0-12-391421-7. doi: 10.1016/B978-0-12-391421-7.00013-0. URL https://www.sciencedirect.com/science/article/pii/B9780123914217000130.

[52] D. G. Crighton, A. P. Dowling, J. E. Ffowcs Williams, M. Heckl, and F. G. Leppington. *Modern Methods in Analytical Acoustics*. Springer, London, 1992. ISBN 978-1-4471-0399-8. doi: 10.1007/978-1-4471-0399-8_16. URL https://doi.org/10.1007/978-1-4471-0399-8_16.

[53] Martin Alnæs, Jan Blechta, Johan Hake, August Johansson, Benjamin Kehlet, Anders Logg, Chris Richardson, Johannes Ring, Marie E. Rognes, and Garth N. Wells. The FEniCS Project Version 1.5. *Archive of Numerical Software*, 3(100), December 2015. ISSN 2197-8263. doi: 10.11588/ans.2015.100.20553. URL https://journals.ub.uni-heidelberg.de/index.php/ans/article/view/20553. Number: 100.

[54] R. L. Pritchard. Mutual Acoustic Impedance between Radiators in an Infinite Rigid Plane. *The Journal of the Acoustical Society of America*, 32(6):730–737, June 1960. ISSN 0001-4966. doi: 10.1121/1.1908199. URL https://asa.scitation.org/doi/10.1121/1.1908199. Publisher: Acoustical Society of America.

[55] Kwai-Cheung Chan. Mutual Acoustic Impedance between Flexible Disks of Different Sizes in an Infinite Rigid Plane. *The Journal of the Acoustical Society of America*, 42(5):1060–1063, November 1967. ISSN 0001-4966. doi: 10.1121/1.1910690. URL https://asa.scitation.org/doi/10.1121/1.1910690. Publisher: Acoustical Society of America.

[56] Thomas Lehrmann Christiansen, Ole Hansen, Erik Vilain Thomsen, and Jørgen Arendt Jensen. Modal radiation patterns of baffled circular plates and membranes. *The Journal of the Acoustical Society of America*, 135(5):2523–2533, May 2014. ISSN 0001-4966. doi: 10.1121/1.4869688. URL https://asa.scitation.org/doi/10.1121/1.4869688. Number: 5 Publisher: Acoustical Society of America.